Original Article

MOLECULAR METABOLISM

$G_s\alpha$ deficiency in the dorsomedial hypothalamus leads to obesity, hyperphagia, and reduced thermogenesis associated with impaired leptin signaling

Min Chen [1,], Eric A. Wilson [1], Zhenzhong Cui [2], Hui Sun [1], Yogendra B. Shrestha [1], Brandon Podyma [1], Christina H. Le [1], Benedetta Naglieri [1], Karel Pacak [3], Oksana Gavrilova [2], Lee S. Weinstein [1,*]**

ABSTRACT

Objective: $G_s\alpha$ couples multiple receptors, including the melanocortin 4 receptor (MC4R), to intracellular cAMP generation. Germline inactivating $G_s\alpha$ mutations lead to obesity in humans and mice. Mice with brain-specific $G_s\alpha$ deficiency also develop obesity with reduced energy expenditure and locomotor activity, and impaired adaptive thermogenesis, but the underlying mechanisms remain unclear.

Methods: We created mice (DMHGsKO) with $G_s\alpha$ deficiency limited to the dorsomedial hypothalamus (DMH) and examined the effects on energy balance and thermogenesis.

Results: DMHGsKO mice developed severe, early-onset obesity associated with hyperphagia and reduced energy expenditure and locomotor activity, along with impaired brown adipose tissue thermogenesis. Studies in mice with loss of MC4R in the DMH suggest that defective DMH MC4R/$G_s\alpha$ signaling contributes to abnormal energy balance but not to abnormal locomotor activity or cold-induced thermogenesis. Instead, DMHGsKO mice had impaired leptin signaling along with increased expression of the leptin signaling inhibitor protein tyrosine phosphatase 1B in the DMH, which likely contributes to the observed hyperphagia and reductions in energy expenditure, locomotor activity, and cold-induced thermogenesis.

Conclusions: DMH $G_s\alpha$ signaling is critical for energy balance, thermogenesis, and leptin signaling. This study provides insight into how distinct signaling pathways can interact to regulate energy homeostasis and temperature regulation.

Keywords G protein; Obesity; Thermogenesis; Hypothalamus; Sympathetic nervous system

1. INTRODUCTION

Monogenic obesity syndromes provide insights into how single genes regulate systemic energy homeostasis. Melanocortin receptor 4 (MC4R) mutations are the most common cause of monogenic obesity and are associated with hyperphagia, reduced energy expenditure, increased body length, and abnormal glucose metabolism [1–3]. Activation of MC4Rs promotes negative energy balance by inhibiting food intake and stimulating energy expenditure [3–6]. MC4Rs can be activated by α-MSH released from POMC neurons in the arcuate nucleus (ARC) of the hypothalamus and couple to the ubiquitously expressed G protein stimulatory α-subunit $G_s\alpha$, encoded by *GNAS* (*Gnas* in mice), to increase intracellular cAMP levels.

In patients with Albright hereditary osteodystrophy (AHO), heterozygous inactivating $G_s\alpha$ mutations lead to obesity, reduced energy expenditure, and increased insulin resistance, but only when the mutation is present on the maternal allele [7–9], and $G_s\alpha$ mutations were shown to lead to a similar parent-of-origin-specific metabolic phenotype in mice [10,11]. We have shown that the parent-of-origin-specific metabolic phenotype is due to *Gnas* imprinting in the central nervous system (CNS) [12], leading to $G_s\alpha$ being primarily expressed from the maternal allele in certain brain areas. Mice with maternal $G_s\alpha$ deficiency in the whole brain (mBrGsKO) develop obesity associated with reduced energy expenditure and impaired stimulation of energy expenditure by an MC4R agonist, while food intake and the ability of an MC4R agonist to inhibit food intake were unaffected [12].

Molecular evidence shows that *Gnas* is imprinted in the paraventricular nucleus (PVN) [12] and the dorsomedial nucleus (DMH) [13], but not in the ventromedial nucleus (VMH) [14], of the hypothalamus. Disruption of the $G_s\alpha$ maternal allele in the DMH

[1]Metabolic Diseases Branch, Bethesda, MD, 20892, USA [2]Mouse Metabolism Core Laboratory, National Institute of Diabetes and Digestive and Kidney Diseases, Bethesda, MD, 20892, USA [3]Section on Medical Neuroendocrinology, Division of Intramural Research, *Eunice Kennedy Shriver* National Institute of Child Health and Human Development, National Institutes of Health, Bethesda, MD, 20892, USA

*Corresponding author. NIDDK/NIH, Bldg 10 Rm 8C101, 10 Center Drive, Bethesda, MD, 20892-1752, USA. E-mail: leew@mail.nih.gov (L.S. Weinstein).

**Corresponding author. NIDDK/NIH, Bldg 10 Rm 8C101, 10 Center Drive, Bethesda, MD, 20892-1752, USA. E-mail: minc@niddk.nih.gov (M. Chen).

Received March 29, 2019 • Accepted April 8, 2019 • Available online 12 April 2019

https://doi.org/10.1016/j.molmet.2019.04.005

(mDMHGsKO) leads to obesity, which is primarily due to reduced energy expenditure [13]. In contrast, disruption of the $G_s\alpha$ maternal allele in VMH [14], PVN [15], or in Agrp neurons [13], or disruption of both $G_s\alpha$ alleles in the VMH [14] or in Pomc neurons (unpublished results) does not lead to obesity. *Gnas* imprinting in the DMH appears to be incomplete as residual $G_s\alpha$ expression ($\sim$30%) could still be detected in the DMH of mice with a maternal germline $G_s\alpha$ deletion [13]. The molecular mechanism by which $G_s\alpha$ in the DMH controls energy balance remains elusive.

The DMH is known to be a key hypothalamic region governing sympathetically mediated adaptive thermogenesis, an important component of energy expenditure [16,17]. Brown adipose tissue (BAT) is one of the major thermogenic organs for adaptive thermogenesis and is largely regulated by sympathetic nervous system (SNS) activity. Adaptive thermogenesis can be induced in response to environmental challenges, such as cold environment or high caloric intake, which are referred to as cold-induced (CIT) and diet-induced thermogenesis (DIT), respectively. The DMH contains neurons that are synaptically connected to BAT via the rostral raphe pallidus (rRPa) and are responsible for increasing SNS outflow to BAT [17–20], leading to stimulation of thermogenesis that is required to maintain body temperature in a cold environment or body weight in response to excess calorie intake. CNS $G_s\alpha$ is involved in the regulation of both CIT and DIT, as both were shown to be impaired in mBrGsKO mice [12,15].

The DMH contains MC4R-expressing neurons [21,22]. The ability of systemic administration of the MC4R agonist melanotan II (MTII) to increase BAT temperature was shown to be attenuated by injection of an MC4R antagonist directly into the DMH, suggesting that MC4R signaling in the DMH may play a role in the regulation of BAT thermogenesis [23]. However, we have recently shown that mice with complete loss of MC4R in the DMH develop obesity associated with decreased energy expenditure but without impairment of CIT [13]. In addition, heterozygotes with maternal $G_s\alpha$ deficiency in the DMH also exhibited normal CIT [13]. It is possible that central MC4R/$G_s\alpha$ signaling in CNS regions outside of the DMH is responsible for the regulation of CIT by melanocortins. However, the consequence of complete loss of $G_s\alpha$ in the DMH on CIT remains unknown. It is also unclear whether $G_s\alpha$ could interact with signaling molecules other than MC4R to regulate adaptive thermogenesis.

In this study, we show that mice with complete $G_s\alpha$ deficiency in the DMH (DMHGsKO) develop severe early-onset obesity associated with hyperphagia, along with decreases in energy expenditure, MTII stimulation of energy expenditure, SNS outflow to BAT, and CIT in response to acute cold exposure. The observed defect in CIT does not appear to be due to impaired MC4R/$G_s\alpha$ signaling in the DMH as DMH-specific loss of MC4R does not impair CIT. Rather, impaired CIT in DMHGsKO mice is associated with impaired leptin signaling in the DMH. In addition, DMHGsKO mice, unlike their heterozygous counterparts, also develop hyperphagia which may also be a result of impaired leptin signaling in the DMH. This study provides novel insights into how crosstalk between divergent signaling pathways in specific hypothalamic nuclei can influence the regulation of energy homeostasis.

2. METHODS

2.1. Generation of mice with homozygous $G_s\alpha$ deficiency in the DMH

We previously generated $G_s\alpha$-floxed mice ($E1^{fl/fl}$) with flox sites surrounding *Gnas* exon 1 [24] and obtained MC4R-floxed ($MC4R^{fl/fl}$) mice as a gift from Brad Lowell (Beth Israel Deaconess Medical Center, Boston, Massachusetts, USA). Male $E1^{fl/fl}$ or $MC4R^{fl/fl}$ mice aged 6–7 weeks were stereotaxically injected bilaterally with either 1.1×10^9 genomic copies/200 nl of AAV-Cre-GFP (AV-2-PV-2004) or 1.4×10^9 AAV-GFP (AV-2-PV0101, Penn Vector Core, Philadelphia, Pennsylvania, USA) into the DMH (bregma: anterio-posterior: −1.88 mm; medio-lateral: ± 0.3 mm; dorso-ventral: −5.125 mm). Injections were performed under isoflurane anesthesia. The correct injection position into the DMH was confirmed by detecting position of GFP expression using fluorescence microscopy (Figure 1A) and, except as noted, only data from mice with correct targeting of viral injection into the DMH bilaterally were used in this study. All mice were maintained on a Black Swiss background, housed on a 12 h light/dark cycle (6 am/6 pm) and fed a standard chow diet (NIH-07, 5% fat by weight, Envigo). Except as noted, all experiments were performed in male mice at 1–3 months post-viral injection (age 2.5–4.5 months). Studies were approved by the NIDDK Animal Care and Use Committee.

2.2. Food intake, body composition, O_2 consumption, and activity

Food intake was measured over a 10-day period during which food was weighed initially and every 2–3 days thereafter. There was minimal food spillage into the cage during these experiments. Body composition was measured in non-anesthetized mice using an EchoMRI 3-in-1 analyzer (Echo Medical Systems). Total energy expenditure (TEE) was determined using a 12-chamber indirect calorimetry system (CLAMS, Columbus Instruments) over a 24 h period at 22 °C after 2 days of adaptation followed by a 24 h period at 30 °C. Resting energy expenditure (REE) was determined as the mean of points measured when the animal was not ambulating. Total and ambulating locomotor activities were determined by infrared beam interruption. Day (light cycle) was 6 am to 6 pm and night (dark cycle) was 6 pm to 6 am. Physical activity was also measured with an E-Mitter mouse telemetry system (Starr Life Science Corp.) using an electronic transponder (G2, E-Mitter) implanted into the abdominal cavity of mice under isoflurane anesthesia.

2.3. MTII injections

For measurement of food intake response to the MC3R/MC4R agonist melanotan II (MTII, Bachem), single-caged mice were fasted for 24 h prior to receiving vehicle (saline, 100 µl i.p.) 30 min before lights out, and food intake was measured over the next 3.5 h (3 h in the dark). Mice were allowed to recover for 2–3 days before a second 24 h fast followed by administration of MTII (200 µg ip) at the same time of day as saline and food intake was again measured over 3.5 h in dark. For energy expenditure response, mice were placed in indirect calorimetry chambers for 24 h at 30 °C and received MTII (10 µg/g i.p.) or vehicle on the following day at 1200 h; crossover treatment was performed 24 h later. Average O_2 consumption was calculated for 3 h before and 3 h after injection, excluding the first hour post-injection.

2.4. Tissue SNS activity

Tissue SNS activity was assessed by measuring DOPA accumulation after inhibiting catecholamine synthesis by blocking L-aromatic amino acid decarboxylase with NSD1015 (100 mg/kg, Sigma) as described previously [25]. To study SNS response to cold, mice were placed at 6 °C for 30 min prior to injection of saline or NSD and kept at 6 °C for another 2 h before tissues were collected. Tissue DOPA content was quantified by reverse phase liquid chromatography.

2.5. Acute cold tolerance and chronic cold adaptation studies

Body temperature was measured using a TH-5 rectal probe (Thermalet, Braintree Scientific) inserted 1 cm deep or with an E-Mitter

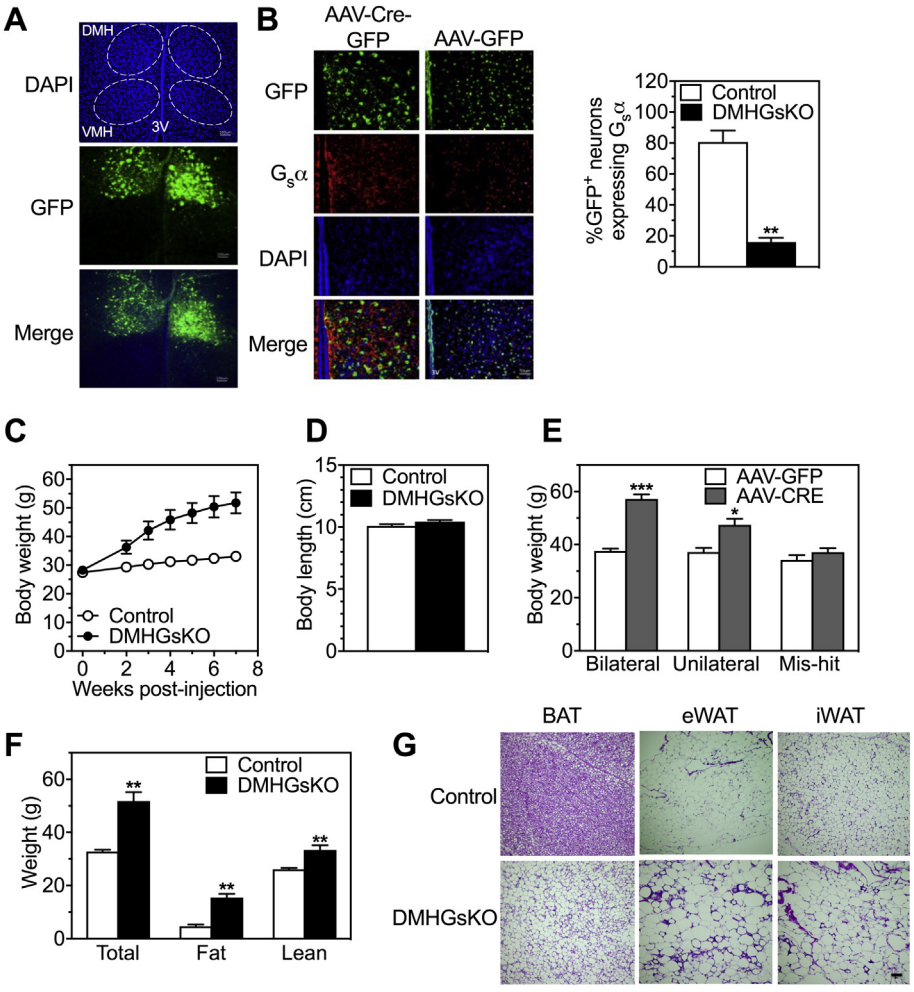

Figure 1: DMHGsKO mice develop obesity. (A) Representative green fluorescence images confirming bilateral injection of AAV-Cre-GFP into the DMH. VMH, ventromedial hypothalamus; 3 V, third ventricle; DAPI, 4′,6-diamidino-2-phenylindole, dihydrochloride (scale bar, 100 μm). (B) Representative images of coimmunofluorescence staining with GFP (green, top) and $G_s\alpha$ protein (red, second row) in the DMH of control and DMHGsKO mice (scale bar, 50 μm). To the right is percent of GFP-expressing cells that are $G_s\alpha^+$, n = 3/group. (C) Body weight curves of male DMHGsKO and control mice post-viral injection, n = 10–11/group. (D) Body length of DMHGsKO and control mice, n = 5–7/group. (E) Body weight of mice at 3–4 months post-viral injection in which AAV-Cre-GFP was correctly targeted to the DMH bilaterally (n = 24–28/group), unilaterally (n = 9–11/group), or neither (mis-hit, n = 6/group). (F) Body composition (total, fat and lean weight) of DMHGsKO and control mice at 15–20 weeks post-injection, n = 10–11/group. (G) Histology (H&E staining) of BAT, epididymal WAT (eWAT) and inguinal WAT (iWAT) adipocytes from DMHGsKO mice and controls (scale bars, 100 μm). *p < 0.05, **p < 0.01, ***p < 0.001 vs. controls. Data represent mean ± S.E.M.

mouse telemetry system using an electronic transponder (G2, E-Mitter, Starr Life Science Corp) implanted into the abdominal cavity of mouse under isoflurane anesthesia. Interscapular BAT (iBAT) temperature was measured using a telemetry temperature probe (IPII-300, Bio Medic Data System) that was surgically implanted into iBAT of mouse under isoflurane anesthesia and detected by a receiver (DAS-7007S, Bio Medic Data System). For acute cold tolerance test, mice were acclimated to experimental conditions at room temperature for 3 days with daily measurement of rectal temperature, and were then caged individually without bedding and provided with food and water *ad libitum*. Rectal and iBAT temperatures were measured hourly before or after exposure to 6 °C for 5 h. For chronic cold adaptation, mice were kept in individual cages with bedding and housed in a climate controlled chamber (Memmert 750 LIFE Chamber) where they were exposed to gradually declining ambient temperatures. Chamber temperature decreased from 22 °C to 6 °C in 2 °C per day increments. Mice were then housed at 6 °C for 5–6 days of the experiment.

2.6. Measurement of heart rate and blood pressure and assessment of body weight at 30 °C

Heart rate and blood pressure were measured with a BP-2000 Specimen platform (Visitech). For measurement of body weight at 30 °C, mice were kept at room temperature for 7 days following stereotaxic viral injections and then housed at 30 °C within a climate controlled chamber (Memmert 750 LIFE Chamber) for 5 weeks.

2.7. RNA analysis

Total RNA was isolated from iBAT using an RNeasy lipid tissue kit (QIAGEN) and treated with DNAse I (Invitrogen) at room temperature for 15 min. Reverse transcription was performed using MultiScribe RT (Applied Biosystems). BAT mRNA levels were measured by quantitative RT-PCR (Applied Biosystems, StepOnePlus) in 20 μl reaction volume, including BAT cDNA (20 ng of initial RNA sample), 50 nM primers and 10 μl of 2x SYBR Green Master Mix (Roche Diagnostics). Results were normalized to simultaneously determined β-actin mRNA levels in each

sample. Expression of BAT genes was quantified using StepOne comparative Ct software and data were presented relative to gene expression of control mice.

2.8. Glucose and insulin tolerance tests

Overnight-fasted mice were administered glucose (2 mg/g ip), or insulin (Humulin, 0.75 mIU/g ip), respectively. In each study tail blood was collected before (time 0) and at indicated times after injection for measurement of glucose using a Glucometer Contour (Bayer).

2.9. Leptin response

Overnight-fasted mice were injected with leptin (5 μg/g ip, R&D Systems) or saline vehicle. After 45 min post-injection, mice were anesthetized with avertin and transcardially perfused with ice-cold PBS followed by ice-cold 4% paraformaldehyde. Brains were removed and post-fixed in 4% paraformaldehyde at 4 °C overnight, and then cryoprotected in 30% sucrose in PBS at 4 °C for 2–3 days. Free floating brain sections (40 μm) were cut using a microtome and brain sections were kept at −80 °C until immunohistochemical analysis.

2.10. Immunohistochemistry

Heat-mediated antigen retrieval was performed on brain sections by incubation in sodium citrate buffer (10 mM sodium citrate, 0.05% Tween 20, pH 6.0) at 95 °C for 30 min prior to immunofluorescent staining. The brain sections were blocked in 2.5% horse serum (Vector Lab) plus 0.3% Triton X-100 at room temperature for 1 h and then incubated with primary antibodies in blocking solution overnight in 4 °C, followed by incubation with Alexa Fluor-conjugated secondary antibodies. The primary antibodies were anti-phopho-STAT3 (Tyr 705; Cell Signaling), anti-PTPase 1B (Ab-1, Oncogene), anti-SOCS-3 (Santa Cruz), anti-GFP (Santa Cruz) and anti-$G_s\alpha$ [26]. The signals in GFP-expressing neurons in the DMH were captured and visualized with fluorescence microscopy. The average on a minimum of 4 sections from each mouse was quantified using BZ-II Analyzer software version 2.1 (Keyence). UCP1 immunohistochemistry was performed as previously described using an anti-UCP1 primary antibody (Abcam, Ab10983, 1:1000 dilution) [27].

2.11. Biochemical assays

Serum insulin and leptin were measured by ELISA (Crystal Chem and R & D Systems, respectively). Serum free fatty acids were measured using Roche Half Micro Test (Sigma), and triglyceride and cholesterol levels were measured using reagents from Thermo Fisher. Serum glucose levels were measured with the Glucometer Contour (Bayer).

2.12. Statistical analysis

Data are expressed as mean ± SEM. Statistical significance was determined by two-tailed unpaired t-test or 2 way ANOVA with differences considered significant at $p < 0.05$.

3. RESULTS

3.1. Mice with DMH-specific $G_s\alpha$ deletion (DMHGsKO) develop severe obesity

We bilaterally injected AAV-Cre-GFP into the DMH of male $G_s\alpha$-floxed mice ($E1^{fl/fl}$) at 6–7 weeks of age. Male $E1^{fl/fl}$ mice that were injected with AAV-GFP served as controls. We confirmed the correct positioning of the stereotaxic injections into the DMH by detection of GFP expression using fluorescence microscopy (Figure 1A). These injections led to an ~85% reduction in GFP-expressing cells within the DMH that also stained for $G_s\alpha$ protein based on immunohistofluorescence (Figure 1B). Mice in which AAV-Cre-GFP injections were targeted correctly on both sides (DMHGsKO mice) gained weight rapidly and were significantly heavier than controls at 2 weeks post-viral injection (Figure 1C), while their body length was unaffected (Figure 1D). At 3–4 months post-viral injection, mice in which the stereotaxic injections of AAV-Cre-GFP hit the correct target (DMH) unilaterally also gained significant more weight than controls, although less than the weight gained by mice in which the injections were correctly targeted bilaterally (Figure 1E). Mice in which the AAV-Cre-GFP injections missed the DMH on both sides showed no difference in body weight compared to controls (Figure 1E). At 15–20 weeks post-viral injection DMHGsKO mice had an ~3-fold increase in fat mass and a smaller but significant increase in lean mass (Figure 1F). Consistent with this finding, we also found circulating leptin levels to be >3-fold higher in DMHGsKO mice compared to controls (Table 1). Histological examination showed DMHGsKO mice to have enlarged adipocytes with greater lipid accumulation per cell in interscapular BAT and epididymal and inguinal white adipose tissue (eWAT and iWAT, respectively; Figure 1G).

3.2. DMHGsKO mice develop hyperphagia

To examine the extent that hyperphagia contributes to the increased weight gain in DMHGsKO mice, we measured food intake in mice over a 10-day period beginning from 7 to 11 days post-viral injection. During this period DMHGsKO mice had a significant weight gain while weight remained stable in controls (Figure 2B). This weight gain disparity was accompanied by a notable increase in food intake in DMHGsKO (Figure 2A), which was not previously observed in heterozygous mDMHGsKO mice [13]. During this period, DMHGsKO mice ate on average ~6.8 kcal/d more than controls, which accounts for virtually all of the greater weight gain (~7.2 g) observed in these mice. Interestingly, the ability of the MC4R agonist MTII to acutely inhibit food intake was unaffected in DMHGsKO mice (Figure 2C), suggesting that the observed hyperphagia may not be secondary to impaired melanocortin action.

3.3. DMHGsKO mice have decreased energy expenditure and physical activity and impaired stimulation of energy expenditure by a melanocortin agonist

We examined resting and total energy expenditure (REE and TEE, respectively) and respiratory exchange ratios (RER; vCO_2/vO_2) by indirect calorimetry, as well as total and ambulatory activity levels, in control and DMHGsKO mice that were raised at 22 °C. Measurements were made over a 24 h period at 22 °C and then at 30 °C (thermoneutrality) over the subsequent 24 h period. The mean weight gains during the time in the calorimetry chamber were not significantly different between groups (control 1.86 ± 0.49 g vs. DMHGsKO 0.60 ± 0.39 g).

When normalized by either total body weight (Figure 2D) or by lean mass (Figure 2E), REE was similar between both groups at

Table 1 — Serum chemistries in control and DMHGsKO mice in fed state at 3–4 months post-viral injection.

	Control	DMHGsKO
Insulin (ng/ml)	4.2 ± 0.9	102.3 ± 33.3**
Free fatty acid (mM)	0.32 ± 0.08	0.22 ± 0.04
Triglyceride (mg/dl)	142 ± 30	228 ± 47*
Leptin (ng/ml)	14.7 ± 2.8	48.4 ± 3.0**
Cholesterol (mg/dl)	172 ± 8	225 ± 20*

Data are presented as mean ± S.E.M. n = 5–7/group. *p < 0.05, **p < 0.01 vs. controls.

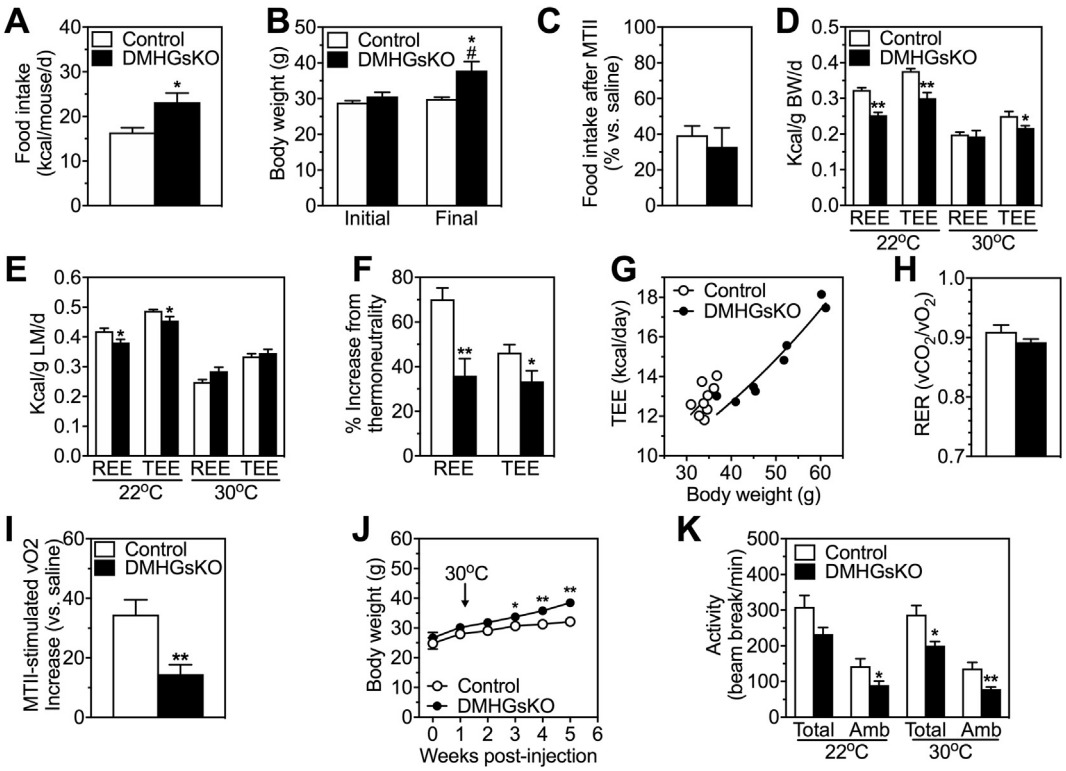

Figure 2: DMHGsKO mice have increased food intake and reduced energy expenditure and physical activity. (A) Mean daily food intake per mouse in DMHGsKO and control mice measured over 10 days starting at 7–11 days post-viral injection, n = 7–8/group. (B) Initial and final mean body weights of mice during the period of food intake measurement in panel A. (C) Total food intake after MTII in DMHGsKO and control mice expressed as % vs. after saline, n = 5–8/group. (D) Energy expenditure (total, TEE, and at rest, REE) measured at 22 °C and 30 °C (thermoneutrality) in DMHGsKO and control mice at 2.5–3 months post-viral injection and normalized by body weight, n = 9/group. Prior to study all mice were maintained at room temperature. (E) Data from experiments in panel D normalized to lean mass. (F) Percent increase in REE and TEE in control and DMHGsKO mice at 22 °C as compared to 30 °C taken from data presented in panels D and E. (G) Plot of daily TEE vs. body weight in individual DMHGsKO and control mice measured at 22 °C with lines indicating exponential fit. (H) Respiratory exchange ratio (vCO_2/vO_2; RER) measured over 24 h at 22 °C, n = 9/group. (I) Percent increase in energy expenditure (O_2 consumption) in response to MTII in DMHGsKO and control mice, n = 9/group. (J) Body weight curves of DMHGsKO and control mice maintained at 30 °C for 4 weeks, n = 10–11/group. (l) Total and ambulatory (Amb) locomotor activity determined by infrared beam interruption, n = 9/group. *p < 0.05, **p < 0.01 vs. controls. #p < 0.05 vs. initial body weight. Data represent mean ± S.E.M.

thermoneutrality (30 °C), a condition in which SNS activity and thermogenesis is minimized. When measured at a temperature below thermoneutrality (22 °C), both REE and TEE were significantly lower in DMHGsKO mice as compared to controls when normalized by total body weight (Figure 2D) or by lean mass (Figure 2E). The percent increase in REE and TEE when measured at 22 °C vs. 30 °C was significantly reduced in DMHGsKO mice as compared to controls (Figure 2F). This finding is independent of the method of normalization and is consistent with DMHGsKO mice having an impaired increase in energy expenditure (thermogenesis) compared to controls in response to a cold environment relative to thermoneutrality. There were no differences in food intake between DMHGsKO and control mice during the calorimetry experiments at either 22 °C or 30 °C when normalized to lean mass (control 0.484 ± 0.026 vs. DMHGsKO 0.493 ± 0.042 kcal/g/d at 22 °C; control 0.398 ± 0.018 vs. DMHGsKO 0.370 ± 0.021 kcal/g/d at 30 °C). A plot of daily TEE at 22 °C vs. body weight for individual mice showed a rightward shift in the exponential curve for DMHGsKO mice, consistent with these mice having reduced TEE at 22 °C (Figure 2G). We observed no differences in the RER between groups at 22 °C (Figure 2H). Consistent with the observed decrease in energy expenditure, acute stimulation of energy expenditure by the melanocortin agonist MTII was significantly impaired in DMHGsKO mice (Figure 2I). As compared to mice raised at 22 °C (Figure 1C), DMHGsKO mice raised at 30 °C showed only a minimal increase in body weight compared to controls with a delayed onset (Figure 2J). Overall, these results are consistent with a disparity in energy expenditure between the two groups that is greater at 22 °C than at 30 °C and are consistent with DMHGsKO mice having impaired stimulation of SNS activity at temperatures below thermoneutrality, leading to reduced energy expenditure and thermogenesis (see below). We also observed that DMHGsKO mice had reduced total and ambulatory activity levels at both 22 °C and 30 °C (Figure 2K; all significant except for total activity at 22 °C). These differences were due to reduced activity levels at nighttime (dark period) while activity levels were not different during the daylight hours (Fig. S1A, B). Core body temperature was also significantly reduced in DMHGsKO mice during the night, while there were no differences in core body temperature between DMHGsKO and control mice during daylight hours (Fig. S1C, D).

3.4. DMHGsKO mice develop insulin-resistance, hyperglycemia, and hyperlipidemia

At 3–4 months post-viral injection, DMHGsKO mice had increased fasting blood glucose (Figure 3A) and serum insulin levels (Figure 3C) compared to control mice and displayed severe glucose intolerance and insulin resistance (Figure 3B,D). Circulating insulin

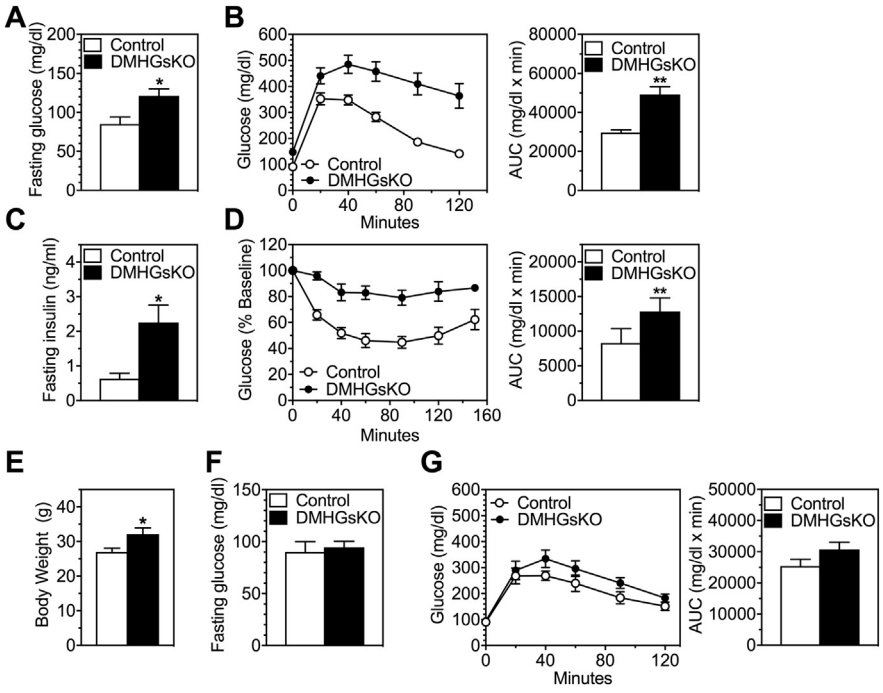

Figure 3: Abnormal glucose metabolism in DMHGsKO mice. (A–D) Glucose metabolism in older mice after development of obesity. (A) Fasting glucose, n = 4–5/group, (B) glucose tolerance tests, n = 9–11/group, (C) fasting insulin levels, n = 4–5/group and (D) insulin tolerance tests in DMHGsKO and control mice at 3–4 months post-viral injection, n = 9/group. For glucose and insulin tolerance tests areas under the curve (AUC) are shown on the right. (E–G) Glucose metabolism at younger age prior to development of severe obesity. (E) Body weight, (F) fasting blood glucose, and (G) glucose tolerance test in mice at 2–3 weeks post-viral injection, n = 6–8/group. *$p < 0.05$, **$p < 0.01$ vs. controls. Data represent mean ± S.E.M.

levels were also markedly elevated in DMHGsKO mice in the fed state (Table 1). We also found these mice to have elevated serum triglyceride and cholesterol levels, although free fatty acids in the fed state were unaffected (Table 1). To determine whether loss of $G_s\alpha$ in the DMH has a direct effect on glucose metabolism independent of obesity, we studied DMHGsKO mice at a younger age (2–3 weeks post-viral injection), when they had a small, but significant, increase in body weight (Figure 3E). At this age we observed no increase in fasting blood glucose in DMHGsKO mice (Figure 3F). Glucose tolerance test showed a trend towards increased glucose levels in DMHGsKO mice at time points 40 min post-glucose administration and beyond, although the areas under the curve for DMHGsKO mice did not differ from those of controls (Figure 3G). Overall, these results indicate that abnormal glucose homeostasis in DMHGsKO mice is primarily secondary to obesity, although we cannot rule out a small direct effect of DMH-specific $G_s\alpha$ on peripheral glucose metabolism.

3.5. DMHGsKO mice have decreased basal and cold-stimulated SNS activity in BAT

To determine whether DMH-specific loss of $G_s\alpha$ affects sympathetic outflow under basal and acute cold conditions, we measured SNS activity in several peripheral tissues of control and DMHGsKO mice kept at room temperature (22 °C) or after cold exposure (6 °C) for 2 h. Tissue SNS activity was assessed by measuring the accumulation of dihydroxyphenylalanine (DOPA) before and after administration of the L-aromatic amino acid decarboxylase inhibitor NSD1015. The increase in accumulation of DOPA after NSD1015 administration is proportional to the rate of catecholamine synthesis and is a reflection of SNS activity [28]. The results showed significantly reduced DOPA accumulation in BAT and heart after NSD1015 administration at 22 °C, indicating reduced basal SNS activity at this temperature in these tissues, while DOPA accumulation in DMHGsKO mice was similar to controls in iWAT, liver and muscle at 22 °C (Figure 4A). After 2 h of cold exposure, DOPA accumulation in heart and liver was similarly augmented in control and DMHGsKO mice, while cold-induced DOPA accumulation was significantly reduced in BAT, iWAT and muscle of DMHGsKO mice (Figure 4A). These results show that DMH $G_s\alpha$ deficiency specifically impairs sympathetic outflow to BAT and heart at 22 °C, and reduces sympathetic outflow to BAT, iWAT and muscle in response to acute exposure to a more extreme cold environment (6 °C). These findings are consistent with the inactive appearance of BAT in DMHGsKO mice based upon histology (Figure 1G). Furthermore, we found reduced expression of genes related to oxidative metabolism and thermogenesis in BAT from DMHGsKO mice, including those encoding PPARγ coactivator 1-α (PGC1-α), cytochrome c oxidase subunit 5B (Cox5b) and 7A (Cox7a), cytochrome C (CytoC), mitochondrial transcription factor (Tfam), PPARγ, adiponectin (Adipoq), and fatty acid binding protein 4 (Fabp4) (Figure 4B). Overall, our results are consistent with reduced SNS activity and activation of BAT in response to cold and a similar finding in iWAT that was more obvious at lower temperature.

DMH neurons are also known to be involved in the regulation of cardiac SNS activity and stress-induced tachycardia via the sympathetic premotor neurons in the rostral medullary raphe region [29,30]. Consistent with reduced basal SNS outflow to heart (Figure 4A) at 22 °C, we observed a reduced heart rate in DMHGsKO mice as compared to controls (Figure 4C), while blood pressure was unaffected (Figure 4D). These results show that $G_s\alpha$ signaling is required for normal regulation of cardiac function via the SNS by DMH neurons.

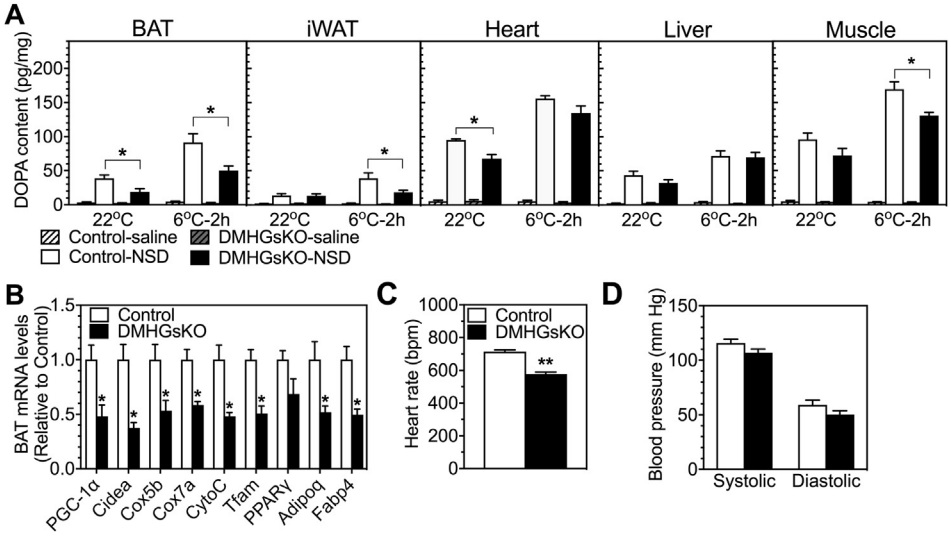

Figure 4: Basal and cold-stimulated SNS activity in adult DMHGsKO mice. (A) Tissue DOPA content in BAT, iWAT, heart, liver and quadriceps muscle of control and DMHGsKO mice injected with either vehicle (saline) or NSD1015 (NSD) when they were kept at room temperature (22 °C) or exposed to cold (6 °C) for 2 h, n = 5–7/group. (B) Relative BAT mRNA levels in DMHGsKO and control mice, n = 6–8/group. (C–D) Cardiovascular function. (C) Heart rate and (D) systolic and diastolic blood pressure in DMHGsKO and control mice, n = 8/group. *p < 0.05, **p < 0.01 vs. controls. Data represent mean ± S.E.M.

3.6. Acute cold tolerance is impaired while adaptation to chronic cold remains intact in DMHGsKO mice

We next examined the acute responses of DMHGsKO and control mice to a cold environment, which requires SNS-stimulated BAT thermogenic function, as well as their adaptation to a chronic cold environment, which may also involve browning of WAT. When acutely exposed to 6 °C for 5 h, DMHGsKO mice showed decreased rectal (Figure 5A) and BAT temperature (Figure 5B). DMHGsKO mice also had significantly reduced basal BAT temperature compared to that of control mice at 22 °C (Figure 5B, 0 time point; control 38.62 ± 0.15 vs. DMHGsKO 37.96 ± 0.17 °C, p < 0.05). Similarly, we observed that BAT *Ucp1* mRNA levels were reduced at 22 °C and further induction of *Ucp1* expression in response to an acute 6 °C environment was significantly attenuated in DMHGsKO mice (Figure 5C). These results are consistent with the reduced SNS activity in BAT at 22 °C and 6 °C that we observed in DMHGsKO mice (Figure 4A).

To test the response to chronic cold adaptation, we placed mice in chambers in which ambient temperature was reduced by 2 °C per day for 8 days, and then maintained at 6 °C for 6 days. In contrast to what we observed during acute cold exposure, DMHGsKO mice were able to maintain their body temperature during the cold adaptation experiment (Figure 5D) and BAT *Ucp1* mRNA levels were induced similarly in DMHGsKO and control mice after chronic cold adaptation (Figure 5C). In addition, we observed that DMHGsKO mice displayed iWAT browning (Figure 5F) with normal induction of UCP1 protein based upon immunohistochemical staining (Figure 5G) as well as *Ucp1* mRNA (Figure 5E) in iWAT after chronic cold adaptation.

We previously showed that, in contrast to DMHGsKO mice, mice with DMH-specific loss of MC4R (DMH-MC4RKO, generated by bilateral stereotaxic injection of AAV-Cre-GFP into the DMH of MC4R$^{fl/fl}$ mice) had normal responses to acute cold (6 °C) conditions, as they were able to maintain normal body temperature and showed normal induction of BAT UCP1 expression, despite also being obese and showing evidence of reduced BAT activation at 22 °C [13]. We now show that, despite their obesity (Fig. S2B), DMH-MC4RKO mice display normal adaptation to chronic cold conditions, as they were able to maintain normal body temperature during chronic cold adaptation experiment (Fig. S2A) and showed normal induction of both BAT *Ucp1* mRNA levels (Fig. S2C) and UCP1 protein in iWAT (Fig. S2D) in response to chronic cold conditions. Overall, these results indicate that DMH $G_s\alpha$ signaling is required for BAT thermogenesis in response to acute cold exposure, but this is not due to loss of MC4R/$G_s\alpha$ signaling in the DMH. Moreover, neither MC4R nor $G_s\alpha$ is required for normal BAT thermogenesis or iWAT browning in response to chronic cold conditions.

3.7. DMHGsKO mice have impaired leptin signaling in the DMH

Studies have shown that DMH neurons express leptin receptors (LepRb) and that leptin signaling in the DMH is involved in the regulation of energy homeostasis by increasing SNS outflow to BAT and stimulating BAT thermogenesis [23,31,32]. To determine whether loss of $G_s\alpha$ affects leptin signaling in the DMH, we measured STAT3 phosphorylation (pSTAT3) in GFP-expressing neurons within the DMH of control and DMHGsKO mice after administration of saline or a single high dose of leptin (5 μg/g ip). Control mice showed significantly increased STAT3 phosphorylation levels in the DMH in response to leptin compared to that of saline-treated controls, while this leptin-induced pSTAT3 was completely absent in the DMH of DMHGsKO mice (Figure 6A,B). In contrast, we observed no significant deficit in leptin-induced STAT3 phosphorylation in non-GFP-expressing (GFP$^-$) cells in the DMH of DMHGsKO mice (Figure 6C). The same deficit in leptin signaling was also observed in the DMH of DMHGsKO mice at 2 weeks post-viral injection at which time these mice had no increase in body weight (Figure 6D), ruling out the possibility that the observed defect in leptin signaling was secondary to obesity. Leptin signaling was specifically impaired in the DMH, as leptin-induced STAT3 phosphorylation in the ARC was unaffected in DMHGsKO mice (Fig. S3B).

Protein tyrosine phosphatase 1B (PTP1B) dephosphorylates Janus-associated kinase 2 (JAK2) to suppress leptin signaling in hypothalamic neurons and regulates body weight [33–35]. Interestingly, we observed that PTP1B levels in the DMH of DMHGsKO mice were

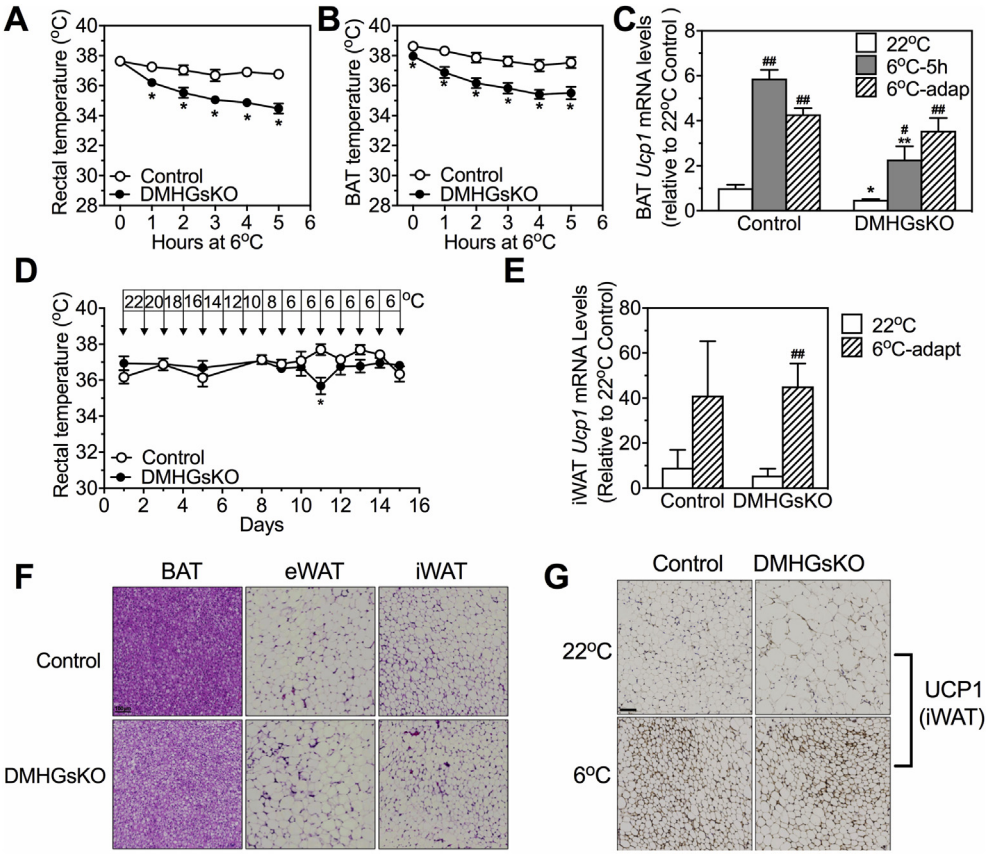

Figure 5: Cold tolerance and adaptation experiments in DMHGsKO mice. (A–C) Acute cold tolerance experiments. (A) Rectal temperature, n = 11–13/group, and (B) BAT temperature, n = 8–9/group, measured during 5 h of cold exposure (6 °C). (C) Relative BAT *Ucp1* mRNA levels in control and DMHGsKO mice that were maintained at 22 °C, exposed to 6 °C for 5 h or that underwent chronic cold adaptation (6°C-adapt), n = 4–7/group. (D–G) Chronic cold-adaptation experiments. (D) Rectal temperature in control and DMHGsKO mice during chronic cold adaptation, n = 6/group. (E) Relative iWAT *Ucp1* mRNA levels in control and DMHGsKO mice at 22 °C or after chronic cold adaptation to 6 °C, n = 3–6/group. (F) Representative histologic images (H&E staining) of BAT, eWAT and iWAT from a DMHGsKO and control mouse after chronic cold adaptation (scale bar, 100 μm). (G) Representative images of immunohistochemical staining for UCP1 in iWAT from a DMHGsKO and control mice maintained at 22 °C or after chronic cold adaptation (scale bar, 100 μm). *$p < 0.05$, **$p < 0.01$ vs. controls. $^{\#}p < 0.05$, $^{\#\#}p < 0.01$ vs. 22 °C. Data represent mean ± S.E.M.

significantly increased (Figure 7). The increase in PTP1B expression appeared to be specifically limited to the DMH of DMHGsKO mice, where $G_s\alpha$ was deleted, as PTP1B levels in the ARC, a region not targeted with AAV-Cre-GFP, were similar in DMHGsKO and control mice (Fig. S3C). Expression of suppressor of cytokine signaling 3 (SOCS3), another known inhibitor of leptin signaling [36,37] was unaffected in the DMH of DMHGsKO mice (Fig. S3A). These results show that loss of $G_s\alpha$ expression leads to impaired leptin signaling in the DMH associated with increased expression levels of the leptin signaling inhibitor PTP1B in the DMH.

4. DISCUSSION

In this study, we show that loss of $G_s\alpha$ signaling in the DMH leads to severe obesity associated with hyperphagia, reduced energy expenditure at temperatures below thermoneutrality, with a minimal effect on glucose metabolism prior to the development of obesity. These manifestations in DMHGsKO mice are likely to be explained to some extent by loss of MC4R action via $G_s\alpha$ in the DMH as we previously showed that DMH-specific loss of MC4R expression also leads to obesity with reduced energy expenditure [13]. Impaired ability of an MC4R agonist to stimulate energy expenditure in either DMHGsKO mice (the present study) or in DMH-MC4RKO mice [13] further confirms that DMH MC4R/$G_s\alpha$ signaling is important for the regulation of energy expenditure. However, we cannot rule out the possibility that loss of MTII action on energy expenditure in DMHGsKO mice could be explained by DMH neurons that are downstream of other MC4R$^+$ neurons in a pathway involved in the regulation of energy expenditure. Also, MTII-stimulated energy expenditure was not completely abrogated in either DMHGsKO mice (this study) or DMH-MC4RKO mice [13], suggesting that other CNS regions may also contribute to melanocortin's actions on energy expenditure.

Our results also demonstrate that $G_s\alpha$ in the DMH has a major effect on food intake. Although we had never previously observed a primary effect on food intake in any of our heterozygous $G_s\alpha$ knockout models, we have recently observed that homozygous loss of $G_s\alpha$ in MC4R-expressing cells leads to significant hyperphagia [27]. However, the effect of DMH-specific $G_s\alpha$ deficiency on food intake is not likely to be due to loss of MC4R/$G_s\alpha$ signaling in DMH, as DMH-specific MC4RKO mice showed no primary changes in food intake [13] and the ability of an MC4R agonist to suppress food intake was unaffected in DMHGsKO mice (this study). Rather we have shown previously that MC4R mediates most of its actions on food intake via $G_{q/11}\alpha$ signaling in the PVN [38]. One possible explanation for the hyperphagia in DMHGsKO is the loss of leptin signaling in DMH (see below).

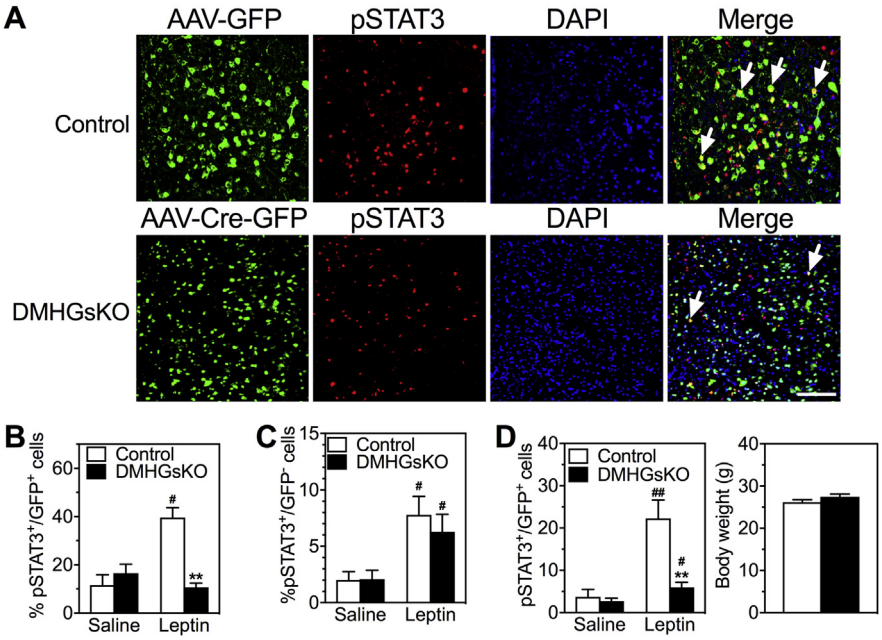

Figure 6: Reduced leptin signaling in the DMH of DMHGsKO mice. (A) Representative images of immunofluorescence for AAV-GFP or AAV-Cre-GFP (green), pSTAT3 (red), DAPI (blue) and merged images after leptin administration in the DMH of DMHGsKO and control mice. Several $pSTAT^+/GFP^+$ cells are indicated with white arrows. (B) Quantification of % GFP^+ cells that were also $pSTAT3^+$ after injection of saline or leptin ip. into control or DMGsKO mice at 3–4 month post-viral injection, n = 4–8/group. (C) Quantification of % GFP^- cells that were also $pSTAT3^+$ after injection of saline or leptin ip., n = 5–6/group. (D) Quantification of % GFP^+ cells that were also $pSTAT3^+$ after injection of saline or leptin ip. into control or DMGsKO mice at 2 weeks post-viral injection while the two groups had similar body weight (body weight shown to the right; n = 6/group). Scale bars, 100 μm. $^{**}p < 0.01$ vs. controls. $^{\#}p < 0.05$, $^{\#\#}p < 0.01$ vs. saline. Data represent mean ± S.E.M.

MC4R/$G_s\alpha$ signaling in the CNS has also been shown to regulate peripheral glucose metabolism independent of its effects on energy balance [12,39,40]. We have shown that loss of $G_s\alpha$ (this study) or MC4R [13] in the DMH had little or no primary effect on peripheral glucose metabolism prior to the onset of obesity. This is consistent with a study showing that the direct glycemic regulatory action of MC4R is most likely controlled by extra-hypothalamic MC4R-expressing neurons, including autonomic neurons [41].

The DMH is a critical site for the control of thermogenesis [16], and it contains neurons that polysynaptically connect to BAT via the rRPa of the brainstem, which includes sympathetic premotor neurons that can be activated by cold to increase BAT SNS activity and thermogenesis [17–20]. We have previously shown that loss of $G_s\alpha$ signaling in the CNS in mBrGsKO mice leads to impaired thermogenesis in response to cold, as these mice are unable to maintain their temperature in a cold environment and have low levels of BAT *Ucp1* mRNA with a markedly reduced response to a cold environment [15]. We now show that loss of $G_s\alpha$ that is limited only to the DMH reproduces the impairment in CIT that we previously observed in mBrGsKO mice, and directly show that DMHGsKO mice have reduced increases in SNS activity in BAT and iWAT in response to acute cold conditions. Consistent with impaired BAT thermogenesis, DMHGsKO mice showed significantly reduced baseline BAT temperature at ambient temperature (22 °C) even though simultaneously measured body temperature no different between DMHGsKO and control mice. However, DMHGsKO mice did not show any impairment in maintaining body temperature or in iWAT browning in response to chronic cold conditions.

Reduced BAT thermogenesis resulting from lower SNS outflow to BAT likely had an impact on the development of obesity in DMHGsKO mice since body weight gain was significantly delayed when these mice were housed at thermoneutral temperature (30 °C), where SNS activity is minimal. Consistent with this, the increase in resting and total energy expenditure observed in control mice at 22 °C relative to 30 °C was significantly reduced in DMHGsKO mice. We also observed a lower heart rate and reduced SNS activity in the heart at 22 °C, consistent with a role for DMH $G_s\alpha$ signaling in cardiovascular regulation.

Studies on the role of MC4R signaling on CIT are inconclusive. Some studies showed that MC4R knockout mice have normal body temperature either at room temperature or after exposure to 4 °C for 1 day [42] or 5 days [42,43]. In contrast, another study showed that MC4R knockout mice have significantly reduced body temperature when maintained at room temperature although this lower body temperature can be maintained when these mice are kept in 4 °C for 5 days [41]. Whether this observation is due to a CIT defect or to a change in the centrally-regulated temperature set point is unclear. In addition, another study showed that BAT UCP1 levels in MC4R knockout mice are normal at room temperature and fail to be stimulated after cold exposure for 1 day but are significantly increased after cold exposure for 5 days [5]. We observed that although DMH-MC4RKO mice develop obesity associated with reduced energy expenditure, they have no defect in CIT under acute [13] or chronic cold conditions (this study). DMH MC4R signaling does play a role in thermogenesis but does not appear to be directly involved in the thermogenic response to cold. Thus, it appears likely that DMH $G_s\alpha$ signaling coordinates with other signaling pathways to mediate the regulation of CIT.

The ability to adapt to chronic cold conditions despite having impaired tolerance to acute cold conditions, which we observed in DMHGsKO mice, have been also observed in other genetically-altered mouse models, including the UCP1 [44–46] and sarcolipin (SLN) knockout models [46]. SLN is proposed to increase thermogenesis in skeletal muscle by uncoupling the sarco(endo)plasmic reticulum Ca^{2+}-ATPase pump leading to heat production. SLN action in muscle [46], along with

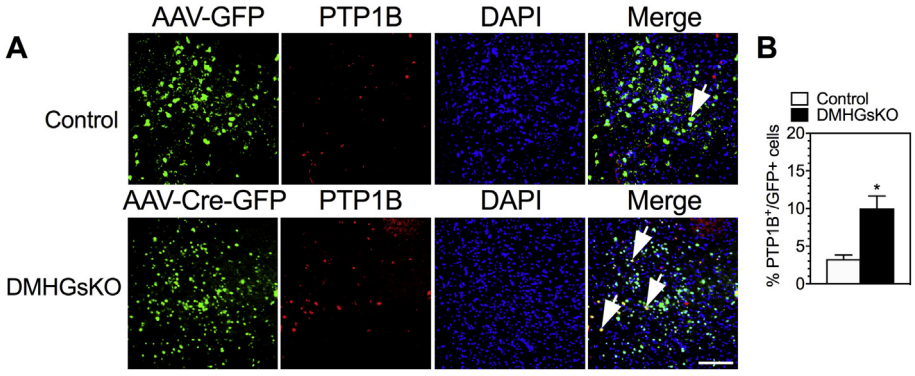

Figure 7: Increased PTP1B expression in DMH of DMHGsKO mice. (A) Representative images of PTP1B expression by immunofluorescence in DMH of 3–4 month-old control and DMHGsKO mice with several PTP1B$^+$/GFP$^+$ cells indicated with arrows. (B) Quantification of % GFP$^+$ cells that were also PTP1B$^+$ in control and DMHGsKO mice, n = 5–7/group. Scale bar, 100 μm. *p < 0.05 vs. controls. Data represent mean ± S.E.M.

UCP1-independent mechanisms in WAT beige adipose tissue [44], have been proposed as compensatory mechanisms to account for the intact adaptation to chronic cold observed in UCP1 knockout mice, and increased BAT thermogenesis and WAT browning can compensate for loss of SLN-mediated thermogenesis [46]. Loss of both UCP1 and SLN led to very poor survival in acute cold. Although we did not look directly at muscle thermogenesis, it is clear that DMHGsKO mice had impaired BAT thermogenesis in response to acute cold. While the extent to which SLN-mediated thermogenesis contributes to the adaptation to chronic cold conditions, our results suggest that long-term both BAT and WAT (in terms of browning) are able to adapt long-term cold conditions.

Leptin is produced by adipocytes and acts through LepRb (leptin receptor)-expressing neurons in several regions of the CNS, including the ARC, DMH, and VMH, to regulate energy balance and glucose homeostasis. We found that the induction of STAT3 phosphorylation in response to leptin observed in the DMH of control mice was absent in DMHGsKO mice. Notably, the impairment of leptin-induced STAT3 phosphorylation occurred only in GFP$^+$ cells, which expressed Cre recombinase, but not in GFP$^-$ cells in the DMH of DMHGsKO mice. In addition, leptin signaling remained intact in the ARC of DMHGsKO, a region in which $G_s\alpha$ was not deleted. The effect of $G_s\alpha$ deficiency on leptin signaling may vary with neuronal subtypes as we previously observed that loss of $G_s\alpha$ in SF1 neurons in the VMH was associated with increased leptin signaling in the setting of diet-induced obesity [14]. Both PTP1B [33–35] and SOCS3 [36,37], known negative regulators of leptin signaling, are overexpressed in the hypothalamus in the setting of obesity and are induced by hyperleptinemia and by inflammation that triggers cellular leptin resistance [36,47]. We observed an ~3-fold increase in PTP1B expression in the DMH of DMHGsKO mice. This is likely related to the loss of $G_s\alpha$ in the DMH and the associated DMH-specific defect in leptin signaling, as we observed no change in PTP1B expression in the ARC of DMHGsKO mice where the $G_s\alpha$ gene was not deleted. In contrast to PTP1B, we found no significant differences in SOCS3 expression in the DMH between DMHGsKO and control mice. Further studies will be required to determine the mechanisms by which $G_s\alpha$ alters PTP1B expression in the DMH and whether mechanisms independent of PTP1B are involved in the reduced leptin signaling that we observed in the DMH of DMHGsKO mice.

Recently LepRb$^+$ neurons that project to the ARC and provide inhibitory GABAergic input to orexigenic Agrp/NPY neurons have been identified in the ventral portion of the DMH [48,49]. Leptin signaling in the DMH appears to regulate food intake as ablation of LepRb in the DMH led to a transient increase in food intake that was observed for only the initial three week period [32]. This effect may be suppressed by the development of obesity, as the ability of leptin to suppress food intake when delivered to the DMH is lost in the setting of obesity [23]. Likewise, we observed DMHGsKO mice to be hyperphagic soon after viral injection before obesity was established, during which time we also documented loss of leptin signaling in the DMH. Therefore loss of loss of leptin signaling in the DMH may underlie the early hyperphagia observed in DMHGsKO mice.

In the DMH, leptin acts through LepRb$^+$ neurons that project directly to the rRPa [31] to enhance thermogenesis by increasing sympathetic input to BAT [23,31,50]. Activation of DMH LepRb$^+$ neurons leads to increased energy expenditure and BAT temperature [32]. While obesity leads to resistance to the effects of leptin on food intake in both ARC and DMH, the action of leptin in the DMH to drive sympathetic outflow to BAT remains intact leading to increased BAT thermogenesis in obese mice, a response that is independent of MC4R [23]. Loss of leptin signaling in the DMH could be responsible for the decreased basal, as well as cold-stimulated, SNS activity in BAT and associated impairment in BAT thermogenesis in DMHGsKO mice. It has been recently reported that leptin's action to maintain body temperature may also involve a decrease in skin thermal conductance [51,52], and this certainly may contribute to the inability of DMHGsKO mice to acutely maintain their body temperature in a cold environment. However, the reduced induction of BAT SNS activity, BAT *Ucp1* expression, and energy expenditure in response to cold, as well as the reduced BAT temperature in sub-thermoneutral temperatures, are all consistent with impaired BAT thermogenesis contributing to the defect in acute temperature regulation.

Another notable observation in this study was that DMHGsKO mice had remarkably reduced locomotor activity, particularly at night, which was accompanied by a lower nighttime core body temperature. While young, non-obese MC4R knockout mice were shown to have significantly reduced locomotor activity [42], locomotor activity in DMH-MC4RKO mice was unaffected [13], suggesting that the reduced locomotor activity in DMHGsKO mice is not due to loss of MC4R signaling in the DMH. Leptin also plays an important role in the regulation of locomotor activity [53], as leptin-deficient ob/ob mice were shown to be hypoactive [54] and the hypoactivity during the dark phase was normalized by leptin administration independent of any effect of leptin on body weight [55]. At least some of the effects of leptin on locomotor activity were shown to be mediated in the ARC [56,57]. However, it has

also been shown that ablation of LepRb in DMH neurons reduces locomotor activity while activation of these DMH neurons stimulates locomotor activity [32], indicating that leptin actions in the DMH also participate in the regulation of locomotor activity. It is therefore likely that impaired leptin signaling in the DMH of DMHGsKO mice significantly contributes to their profoundly reduced locomotor activity.

5. CONCLUSION

DMH-specific $G_s\alpha$ deficiency results in early-onset obesity associated with hyperphagia and decreased energy expenditure and locomotor activity, along with diminished SNS outflow and activation of BAT thermogenesis, particularly in response to cold. While loss of MC4R action in the DMH likely contributes to the abnormal energy balance observed in these mice, impaired leptin signaling in the DMH also contributes to impaired energy balance as well as to BAT thermogenesis in response to cold and to locomotor activity. The present study provides insight into how interactions between seemingly unrelated signaling pathways in specific hypothalamic nuclei contribute to the regulation of energy homeostasis and temperature regulation.

AUTHOR CONTRIBUTIONS

M.C. and L.S.W. conceived the project and directed the study with input from all authors. M.C., Y.B.S., O.G., and L.S.W. were involved in design of experiments. M.C., E.A.W., Z.C., Y.B.S, B.P., H.S., B.N., K.P., C.H.L., and O.G. performed the experiments. M.C., E.A.W., K.P., O.G., C.H.L., and L.S.W. were involved in data analysis. M.C. and L.S.W. wrote the manuscript, and all authors were involved in review and editing of the manuscript.

ACKNOWLEDGMENTS

We would like to thank Thanh Huynh, Yinyan Ma, and Naili Liu for technique assistance and Brad Lowell for providing MC4R-floxed mice. This study was supported by the Intramural Research Programs of the National Institute of Diabetes and Digestive and Kidney Diseases and the Eunice Shriver National Institute of Child Health and Human Development, National Institutes of Health, Bethesda, Maryland, USA.

CONFLICT OF INTEREST

None declared.

APPENDIX A. SUPPLEMENTARY DATA

Supplementary data to this article can be found online at https://doi.org/10.1016/j.molmet.2019.04.005.

REFERENCES

[1] Huszar, D., Lynch, C.A., Fairchild-Huntress, V., Dunmore, J.H., Fang, Q., Berkemeier, L.R., et al., 1997. Targeted disruption of the melanocortin-4 receptor results in obesity in mice. Cell 88:131–141.

[2] Farooqi, I.S., Keogh, J.M., Yeo, G.S., Lank, E.J., Cheetham, T., O'Rahilly, S., 2003. Clinical spectrum of obesity and mutations in the melanocortin 4 receptor gene. New England Journal of Medicine 348:1085–1095.

[3] Fan, W., Morrison, S.F., Cao, W.H., Yu, P., 2007. Thermogenesis activated by central melanocortin signaling is dependent on neurons in the rostral raphe pallidus (rRpa) area. Brain Research 1179:61–619.

[4] Butler, A.A., Cone, R.D., 2002. The melanocortin receptors: lessons from knockout models. Neuropeptides 36:77–84.

[5] Voss-Andreae, A., Murphy, J.G., Ellacott, K.L., Stuart, R.C., Nillni, E.A., Cone, R.D., et al., 2007. Role of the central melanocortin circuitry in adaptive thermogenesis of brown adipose tissue. Endocrinology 148:1550–1560.

[6] Yasuda, T., Masaki, T., Kakuma, T., Yoshimatsu, H., 2004. Hypothalamic melanocortin system regulates sympathetic nerve activity in brown adipose tissue. Experimental Biology and Medicine (Maywood) 229:235–239.

[7] Long, D.N., McGuire, S., Levine, M.A., Weinstein, L.S., Germain-Lee, E.L., 2007. Body mass index differences in pseudohypoparathyroidism type 1a versus pseudopseudohypoparathyroidism may implicate paternal imprinting of $G_s\alpha$ in the development of human obesity. Journal of Clinical Endocrinology & Metabolism 92:1073–1079.

[8] Roizen, J.D., Danzig, J., Groleau, V., McCormack, S., Casella, A., Harrington, J., et al., 2016. Resting energy expenditure is decreased in pseudohypoparathyroidism type 1a. Journal of Clinical Endocrinology & Metabolism 101:880–888.

[9] Muniyappa, R., Warren, M.A., Zhao, X., Aney, S.C., Courville, A.B., Chen, K.Y., et al., 2013. Reduced insulin sensitivity in adults with pseudohypoparathyroidism type 1a. Journal of Clinical Endocrinology & Metabolism 98:E1796–E1801.

[10] Chen, M., Gavrilova, O., Liu, J., Xie, T., Deng, C., Nguyen, A.T., et al., 2005. Alternative *Gnas* gene products have opposite effects on glucose and lipid metabolism. Proceedings of the National Academy of Sciences of the United States of America 102:7386–7391.

[11] Germain-Lee, E.L., Schwindinger, W., Crane, J.L., Zewdu, R., Zweifel, L.S., Wand, G., et al., 2005. A mouse model of Albright hereditary osteodystrophy generated by targeted disruption of exon 1 of the *Gnas* gene. Endocrinology 146:4697–4709.

[12] Chen, M., Wang, J., Dickerson, K.E., Kelleher, J., Xie, T., Gupta, D., et al., 2009. Central nervous system imprinting of the G protein $G_s\alpha$ and its role in metabolic regulation. Cell Metabolism 9:548–555.

[13] Chen, M., Shrestha, Y.B., Podyma, B., Cui, Z., Naglieri, B., Sun, H., et al., 2017. $G_s\alpha$ deficiency in the dorsomedial hypothalamus underlies obesity associated with $G_s\alpha$ mutations. Journal of Clinical Investigation 127:500–510.

[14] Berger, A., Kablan, A., Yao, C., Ho, T., Podyma, B., Weinstein, L.S., et al., 2016. $G_s\alpha$ deficiency in the ventromedial hypothalamus enhances leptin sensitivity and improves glucose homeostasis in mice on a high-fat diet. Endocrinology 157:600–610.

[15] Chen, M., Berger, A., Kablan, A., Zhang, J., Gavrilova, O., Weinstein, L.S., 2012. $G_s\alpha$ deficiency in the paraventricular nucleus of the hypothalamus partially contributes to obesity associated with $G_s\alpha$ mutations. Endocrinology 153:4256–4265.

[16] Dimicco, J.A., Zaretsky, D.V., 2007. The dorsomedial hypothalamus: a new player in thermoregulation. American Journal of Physiology Regulatory Integrative and Comparative Physiology 292:R47–R63.

[17] Morrison, S.F., Madden, C.J., Tupone, D., 2014. Central neural regulation of brown adipose tissue thermogenesis and energy expenditure. Cell Metabolism 19:741–756.

[18] Hosoya, Y., Ito, R., Kohno, K., 1987. The topographical organization of neurons in the dorsal hypothalamic area that project to the spinal cord or to the nucleus raphe pallidus in the rat. Experimental Brain Research 66:500–506.

[19] Nakamura, K., Matsumura, K., Hubschle, T., Nakamura, Y., Hioki, H., Fujiyama, F., et al., 2004. Identification of sympathetic premotor neurons in medullary raphe regions mediating fever and other thermoregulatory functions. Journal of Neuroscience 24:5370–5380.

[20] Cao, W.H., Fan, W., Morrison, S.F., 2004. Medullary pathways mediating specific sympathetic responses to activation of dorsomedial hypothalamus. Neuroscience 126:229–240.

[21] Kishi, T., Aschkenasi, C.J., Lee, C.E., Mountjoy, K.G., Saper, C.B., Elmquist, J.K., 2003. Expression of melanocortin 4 receptor mRNA in the

central nervous system of the rat. Journal of Comparative Neurology 457: 213–235.

[22] Mountjoy, K.G., Mortrud, M.T., Low, M.J., Simerly, R.B., Cone, R.D., 1994. Localization of the melanocortin-4 receptor (MC4-R) in neuroendocrine and autonomic control circuits in the brain. Molecular Endocrinology 8:1298–1308.

[23] Enriori, P.J., Sinnayah, P., Simonds, S.E., Garcia Rudaz, C., Cowley, M.A., 2011. Leptin action in the dorsomedial hypothalamus increases sympathetic tone to brown adipose tissue in spite of systemic leptin resistance. Journal of Neuroscience 31:12189–12197.

[24] Chen, M., Gavrilova, O., Zhao, W.Q., Nguyen, A., Lorenzo, J., Shen, L., et al., 2005. Increased glucose tolerance and reduced adiposity in the absence of fasting hypoglycemia in mice with liver-specific $G_s\alpha$ deficiency. Journal of Clinical Investigation 115:3217–3227.

[25] Chen, M., Chen, H., Nguyen, A., Gupta, D., Wang, J., Lai, E.W., et al., 2010. $G_s\alpha$ deficiency in adipose tissue leads to a lean phenotype with divergent effects on cold tolerance and diet-induced thermogenesis. Cell Metabolism 11: 320–330.

[26] Simonds, W.F., Goldsmith, P.K., Woodard, C.J., Unson, C.G., Spiegel, A.M., 1989. Receptor and effector interactions of Gs. Functional studies with antibodies to the α_s carboxyl-terminal decapeptide. FEBS Letters 249:189–194.

[27] Podyma, B., Sun, H., Wilson, E.A., Carlson, B., Pritikin, E., Gavrilova, O., et al., 2018. The stimulatory G protein $G_s\alpha$ is required in melanocortin 4 receptor-expressing cells for normal energy balance, thermogenesis, and glucose metabolism. Journal of Biological Chemistry 293:10993–11005.

[28] Pacak, K., Palkovits, M., Kvetnansky, R., Matern, P., Hart, C., Kopin, I.J., et al., 1995. Catecholaminergic inhibition by hypercortisolemia in the paraventricular nucleus of conscious rats. Endocrinology 136:4814–4819.

[29] Samuels, B.C., Zaretsky, D.V., DiMicco, J.A., 2002. Tachycardia evoked by disinhibition of the dorsomedial hypothalamus in rats is mediated through medullary raphe. Journal of Physiology 538:941–946.

[30] Cao, W.H., Morrison, S.F., 2003. Disinhibition of rostral raphe pallidus neurons increases cardiac sympathetic nerve activity and heart rate. Brain Research 980:1–10.

[31] Zhang, Y., Kerman, I.A., Laque, A., Nguyen, P., Faouzi, M., Louis, G.W., et al., 2011. Leptin-receptor-expressing neurons in the dorsomedial hypothalamus and median preoptic area regulate sympathetic brown adipose tissue circuits. Journal of Neuroscience 31:1873–1884.

[32] Rezai-Zadeh, K., Yu, S., Jiang, Y., Laque, A., Schwartzenburg, C., Morrison, C.D., et al., 2014. Leptin receptor neurons in the dorsomedial hypothalamus are key regulators of energy expenditure and body weight, but not food intake. Molecular Metabolism 3:681–693.

[33] Bence, K.K., Delibegovic, M., Xue, B., Gorgun, C.Z., Hotamisligil, G.S., Neel, B.G., et al., 2006. Neuronal PTP1B regulates body weight, adiposity and leptin action. Nature Medicine 12:917–924.

[34] Tsou, R.C., Rak, K.S., Zimmer, D.J., Bence, K.K., 2014. Improved metabolic phenotype of hypothalamic PTP1B-deficiency is dependent upon the leptin receptor. Molecular Metabolism 3:301–312.

[35] Zabolotny, J.M., Bence-Hanulec, K.K., Stricker-Krongrad, A., Haj, F., Wang, Y., Minokoshi, Y., et al., 2002. PTP1B regulates leptin signal transduction in vivo. Developmental Cell 2:489–495.

[36] Bjorbaek, C., Elmquist, J.K., Frantz, J.D., Shoelson, S.E., Flier, J.S., 1998. Identification of SOCS-3 as a potential mediator of central leptin resistance. Molecular Cell 1:619–625.

[37] Mori, H., Hanada, R., Hanada, T., Aki, D., Mashima, R., Nishinakamura, H., et al., 2004. Socs3 deficiency in the brain elevates leptin sensitivity and confers resistance to diet-induced obesity. Nature Medicine 10:739–743.

[38] Li, Y.Q., Shrestha, Y., Pandey, M., Chen, M., Kablan, A., Gavrilova, O., et al., 2016. $G_{q/11}\alpha$ and $G_s\alpha$ mediate distinct physiological responses to central melanocortins. Journal of Clinical Investigation 126:40–49.

[39] Fan, W., Dinulescu, D.M., Butler, A.A., Zhou, J., Marks, D.L., Cone, R.D., 2000. The central melanocortin system can directly regulate serum insulin levels. Endocrinology 141:3072–3079.

[40] Obici, S., Feng, Z., Tan, J., Liu, L., Karkanias, G., Rossetti, L., 2001. Central melanocortin receptors regulate insulin action. Journal of Clinical Investigation 108:1079–1085.

[41] Berglund, E.D., Liu, T., Kong, X., Sohn, J.W., Vong, L., Deng, Z., et al., 2014. Melanocortin 4 receptors in autonomic neurons regulate thermogenesis and glycemia. Nature Neuroscience 17:911–913.

[42] Ste Marie, L., Miura, G.I., Marsh, D.J., Yagaloff, K., Palmiter, R.D., 2000. A metabolic defect promotes obesity in mice lacking melanocortin-4 receptors. Proceedings of the National Academy of Sciences of the United States of America 97:12339–12344.

[43] Butler, A.A., Marks, D.L., Fan, W., Kuhn, C.M., Bartolome, M., Cone, R.D., 2001. Melanocortin-4 receptor is required for acute homeostatic responses to increased dietary fat. Nature Neuroscience 4:605–611.

[44] Ukropec, J., Anunciado, R.P., Ravussin, Y., Hulver, M.W., Kozak, L.P., 2006. Ucp1-independent thermogenesis in white adipose tissue of cold-acclimated *Ucp1*$^{-/-}$ mice. Journal of Biological Chemistry 281:31894–31908.

[45] Ukropec, J., Anunciado, R.V., Ravussin, Y., Kozak, L.P., 2006. Leptin is required for uncoupling protein-1-independent thermogenesis during cold stress. Endocrinology 147:2468–2480.

[46] Rowland, L.A., Bal, N.C., Kozak, L.P., Periasamy, M., 2015. Uncoupling protein 1 and sarcolipin are required to maintain optimal thermogenesis, and loss of both systems compromises survival of mice under cold stress. Journal of Biological Chemistry 290:12282–12289.

[47] Zabolotny, J.M., Kim, Y.B., Welsh, L.A., Kershaw, E.E., Neel, B.G., Kahn, B.B., 2008. Protein-tyrosine phosphatase 1b expression is induced by inflammation in vivo. Journal of Biological Chemistry 283:14230–14241.

[48] Garfield, A.S., Shah, B.P., Burgess, C.R., Li, M.M., Li, C., Steger, J.S., et al., 2016. Dynamic GABAergic afferent modulation of AgRP neurons. Nature Neuroscience 19:1628–1635.

[49] Xu, J., Bartolome, C.L., Low, C.S., Yi, X., Chien, C.H., Wang, P., et al., 2018. Genetic identification of leptin neural circuits in energy and glucose homeostases. Nature 556:505–509.

[50] Dodd, G.T., Worth, A.A., Nunn, N., Korpal, A.K., Bechtold, D.A., Allison, M.B., et al., 2014. The thermogenic effect of leptin is dependent on a distinct population of prolactin-releasing peptide neurons in the dorsomedial hypothalamus. Cell Metabolism 20:639–649.

[51] Fischer, A.W., Hoefig, C.S., Abreu-Vieira, G., de Jong, J.M.A., Petrovic, N., Mittag, J., et al., 2016. Leptin raises defended body temperature without activating thermogenesis. Cell Reports 14:1621–1631.

[52] Kaiyala, K.J., Ogimoto, K., Nelson, J.T., Muta, K., Morton, G.J., 2016. Physiological role for leptin in the control of thermal conductance. Molecular Metabolism 5:892–902.

[53] Ceccarini, G., Maffei, M., Vitti, P., Santini, F., 2015. Fuel homeostasis and locomotor behavior: role of leptin and melanocortin pathways. Journal of Endocrinological Investigation 38:125–131.

[54] Mayer, J., 1953. Decreased activity and energy balance in the hereditary obesity-diabetes syndrome of mice. Science 117:504–505.

[55] Ribeiro, A.C., Ceccarini, G., Dupre, C., Friedman, J.M., Pfaff, D.W., Mark, A.L., 2011. Contrasting effects of leptin on food anticipatory and total locomotor activity. PLoS One 6:e23364.

[56] Coppari, R., Ichinose, M., Lee, C.E., Pullen, A.E., Kenny, C.D., McGovern, R.A., et al., 2005. The hypothalamic arcuate nucleus: a key site for mediating leptin's effects on glucose homeostasis and locomotor activity. Cell Metabolism 1:63–72.

[57] Huo, L., Gamber, K., Greeley, S., Silva, J., Huntoon, N., Leng, X.H., et al., 2009. Leptin-dependent control of glucose balance and locomotor activity by POMC neurons. Cell Metabolism 9:537–547.

